Climate Dynamics
https://doi.org/10.1007/s00382-020-05386-0

Surface mean temperature from the observational stations and multiple reanalyses over the Tibetan Plateau

Yuping Yan[1] · Qinglong You[2] · Fangying Wu[3] · Nick Pepin[4] · Shichang Kang[5,6]

Received: 8 May 2020 / Accepted: 21 July 2020

Abstract
The Tibetan Plateau (TP), also called the "Third pole", is sensitive to climate change due to extensive areas at high elevation presently dominated by snow and ice. In this study, observed surface temperature trends at 150 stations over the TP during 1979–2018 are analyzed and compared with surface temperatures from multiple reanalyses (NCEP1, NCEP2, ERA-Interim, MERRA, JRA55). Observed warming at the stations has a mean annual rate of 0.46 °C/decade during 1979–2018. Although all reanalyses underestimate observed temperatures (cold bias), most reproduce much of the inter-decadal variations of surface temperature shown in the observations. Absolute errors of mean surface temperature (reanalysis minus observation) are closely correlated with elevation errors, suggesting that parts of the cold bias can be interpreted by elevation errors of reanalysis. After elevation-temperature correction, about half of the cold bias is typically eliminated, more for both ERA-Interim and JRA55. Compared with the observations, corrected NCEP2 surface temperatures still have larger cold biases, and fail to capture the overall warming over the TP. Since the elevation-temperature correction fails to improve trend magnitudes even when a significant proportion of the bias has been removed, this suggests that a more sophisticated modeling of the lapse rate in each reanalysis is required to realistically model warming trends across complex topography.

Keywords Tibetan Plateau · Elevation correction · Multiple reanalysis · Surface mean temperature

1 Introduction

The Tibetan Plateau (TP hereafter), with an average elevation of over 4000 m, is the highest and the largest highland in the world, which is thus called the "Third Pole". It also contains the largest cryospheric region (snow cover, ice and glaciers, permafrost) outside the polar regions, and has been referred to as the "Asian water tower" (Duan and Xiao 2015; Immerzeel et al. 2010; Kang et al. 2010, 2019; Qiu 2008; Smith and Bookhagen 2018; Yang et al. 2019; Yao et al. 2012, 2019; You et al. 2020b). Due to unprecedented warming, the cryosphere has seen rapid shrunk during recent decades, including in the so-called "global warming hiatus" period, and this has had significant environmental consequences (Ji and Kang 2013a; Kang et al. 2010, 2019; Kuang and Jiao 2016; You et al. 2013, 2016, 2017, 2020b). For example, the retreat of glaciers and thaw of permafrost have resulted in the loss of water content, with serious environmental implications (Qiu 2008; Yang et al. 2019; Yao et al. 2019).

The more pronounced warming over the TP and its physical explanations have been described extensively in

✉ Qinglong You
qlyou@fudan.edu.cn; yqingl@126.com

1 National Climate Center, China Meteorological Administration, Beijing 100081, China

2 Department of Atmospheric and Oceanic Sciences and Institute of Atmospheric Science, Fudan University, Room 5002-1, Environmental Science Building, No. 2005 Songhu Road, Yangpu, Shanghai 200438, China

3 Key Laboratory of Meteorological Disaster, Ministry of Education (KLME), Nanjing University of Information Science and Technology (NUIST), Nanjing 210044, China

4 Department of Geography, University of Portsmouth, Portsmouth PO1 2UP, UK

5 State key Laboratory of Cryospheric Science, Northwest Institute of Eco-Environment and Resources, Chinese Academy of Sciences (CAS), Lanzhou 730000, China

6 CAS Center for Excellence in Tibetan Plateau Earth Sciences, Beijing 100101, China

Published online: 29 July 2020

previous studies based on the observational data (Liu et al. 2006, 2009; Yan and Liu 2014; Yao et al. 2019; You et al. 2016), remote sensing dataset (Cai et al. 2017; Qin et al. 2009), reanalyses (Gao et al. 2012, 2017; Zhao et al. 2008; Zou et al. 2014) and numerical climate model output (Guo et al. 2016a; Ji and Kang 2013a, b; You et al. 2016, 2019a). In modeling studies, the rapid warming over the TP is an intrinsic feature of future global warming scenarios of 1.5 °C and 2 °C relative to the pre-industrial period, particularly so at the higher threshold (You et al. 2019a). However, there is limited coverage of observations over the western TP and higher elevations (> 4000 m), and the demand for high-quality, high-resolution and long-range climate data has become particularly urgent over the TP. Reanalysis referred as a global common source of data, plays an extremely important role in the field of atmospheric science, and provides a powerful research dataset for understanding the laws of atmospheric movement, global and regional climate change and variability (Kalnay et al. 1996; Kanamitsu et al. 2002).

People have little understanding of the climatic characteristics and the reliability of the reanalysis data in the study of climate change in the high mountain areas of the TP (Frauenfeld et al. 2005; Ma et al. 2008; Song et al. 2016; You et al. 2013). There are few detailed comparisons of robust warming in the many reanalyses now available for the TP region (You et al. 2010a, 2013, 2016), and the application of reanalyses over the TP can extend the comprehensive understanding of climate change over the region. The previous

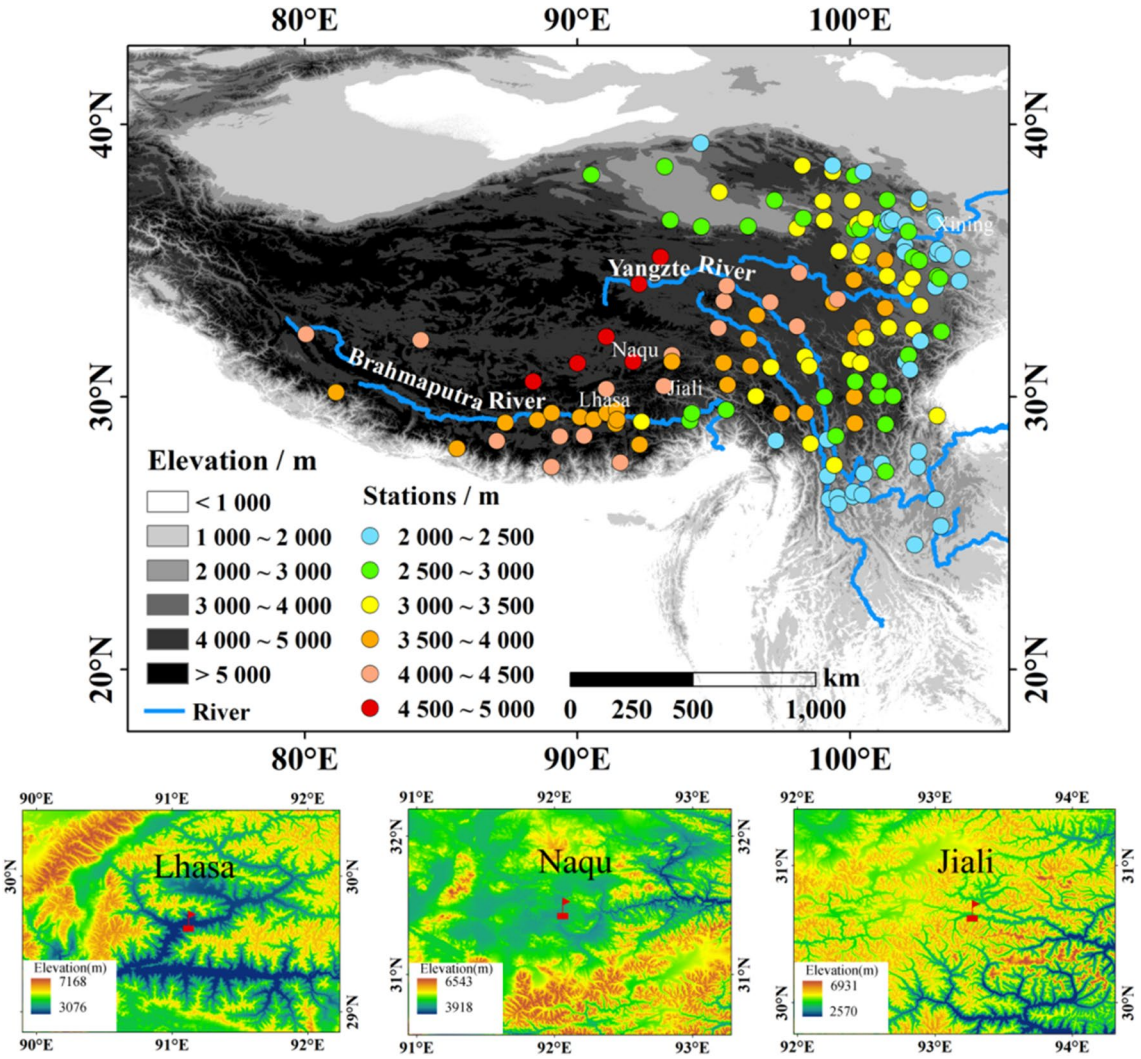

Fig. 1 The distribution of 150 stations with elevation information over the Tibetan Plateau. The 150 stations were classified into 3 topographic types: summit, flat and valley stations, according to a topographical index defined by the elevation difference between the station and the eight surrounding cells derived from GTOPO30 digital elevation data (available from at n://eros.usgs.gov) (You et al. 2008b). Most stations over the Tibetan Plateau are classified as valley or flat stations. Lhasa (WMO No. 55591), Naqu (WMO No. 55299) and Jiali (WMO No. 56202) are examples of valley, flat and summit stations, respectively. WMO is World Meteorological Organization

study (You et al. 2013) has illustrated cold biases (in comparison with the observations) for NCEP/NCAR and ERA-40 reanalyses over the TP during 1961–2004. In part this is due to differing elevations between stations and reanalysis grid points, suggesting that elevation-correction is essential before application to trend analysis (Gao et al. 2017; Guo et al. 2016b; Simmons et al. 2004; Song et al. 2016). Nevertheless, the elevation-correction of the multiple reanalyses and the overall assessments of these datasets over the TP are still lacked.

In this study, the recent warming of surface mean temperature over the TP is analyzed both from updated station observations and multiple reanalyses performed by the elevation-correction. The purpose of study is to address two issues: (1) How well do the modern reanalyses reproduce the observed warming and its warming signature over the

Table 1 Summary of the observations and reanalyses used in this study

Name	Organization	Temporal resolution	Horizontal resolution	Pressure levels	Sources	References
NCEP1	NCEP/NCAR	1948–2018	2.5°×2.5°	17	http://www.esrl.noaa.gov	Kalnay et al. (1996)
NCEP2	NCEP/DOE	1979–2018	2.5°×2.5°	17	http://www.esrl.noaa.gov	Kanamitsu et al. (2002)
ERA-Interim	ECMWF	1979–2018	1°×1°	37	http://www.ecmwf.int	Dee et al. (2011)
MERRA	NASA GMAO	1979–2018	0.5°×0.625°	42	http://disc.sci.gsfc.nasa.gov	Rienecker et al. (2011)
JRA55	JMA	1958–2018	1.25°×1.25°	37	http://jra.kishou.go.jp	Kobayashi et al. (2015)
Observation	CMA	1979–2018	Stations		http://www.cma.gov.cn	Li et al. (2014), Xu et al. (2009)

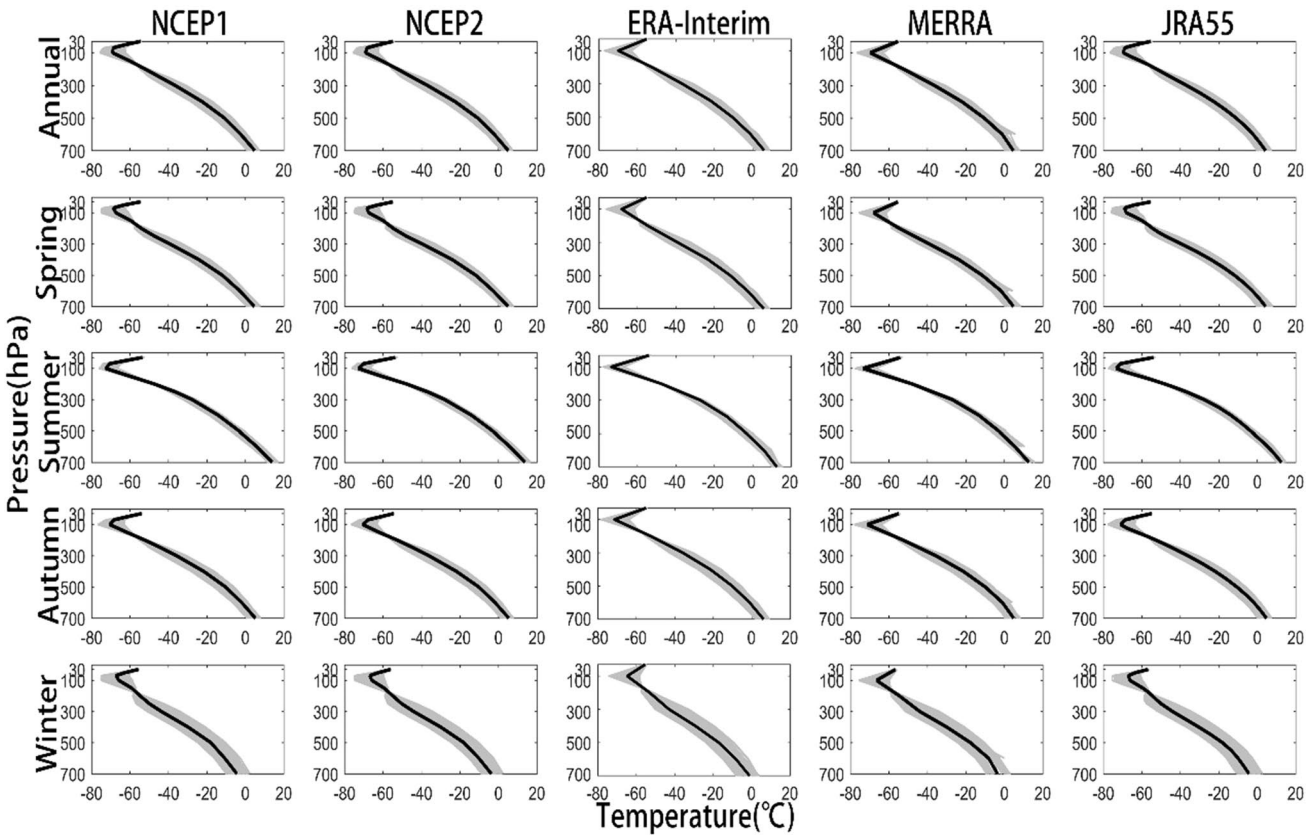

Fig. 2 Mean temperature profiles from multiple reanalyses (NCEP1, NCEP2, ERA-Interim, MERRA and JRA55) over the Tibetan Plateau during 1979–2018 on an annual and seasonal basis. The black curve within each panel represents the mean of 150 temperature profiles interpolated in each reanalysis (shaded). The mean profile varied by stations and periods is used to calculate representative lapse rates on an annual basis and for the four seasons, later used in reanalysis correction

TP? (2) Can the elevation-correction for reanalyses reduce the differences between the observations and reanalyses? Understanding of these issues will lead to a more comprehensive appreciation of the reliability and quantification of modern reanalyses in high elevation regions such as the TP.

2 Data and methods

Observed monthly mean surface temperature at 150 stations (Fig. 1) is provided by the National Meteorological Information Center, China Meteorological Administration (NMIC/CMA) (Li et al. 2014; Xu et al. 2009). Data quality of the observations is checked by a procedure, which can identify a first erroneous value, and the details are described in previous papers (You et al. 2008a, b). For example, 3 standard deviations of the time series are used as the thresholds to check the outliers of the dataset. The majority of stations over the TP belong to valley or flat stations (Fig. 1). Only stations above 2000 m a.s.l. with complete data for 1979–2018 were selected.

Monthly surface air temperatures (2 m above ground level) from five modern reanalyses are used. These include the National Centers for Environmental Prediction (NCEP)-National Center for Atmospheric Research (NCAR) Reanalysis Project (NCEP1) (Kalnay et al. 1996; Kistler et al. 2001); the NCEP-Department of Energy (DOE) Reanalysis Project (NCEP2) (Kanamitsu et al. 2002); the European Centre for Medium-Range Weather Forecasts (ECMWF) Interim Reanalysis (ERA-Interim) (Dee et al. 2011); the Japan Meteorological Agency (JMA) 55 year Reanalysis Project (JRA55) (Kobayashi et al. 2015); and the National Aeronautics and Space Administration (NASA) Modern-Era Retrospective Analysis for Research and Applications (MERRA) (Rienecker et al. 2011). The details of the observations and multiple reanalyses are summarized in Table 1.

To account for differences between station observations and each reanalysis, elevation analysis is performed. The real elevation of each surface station (provided by NMI/CMA) is compared with the model elevation of each reanalysis (interpolated from the nearest four grid points). To ensure a fair comparison, we interpolated the reanalysis temperature to

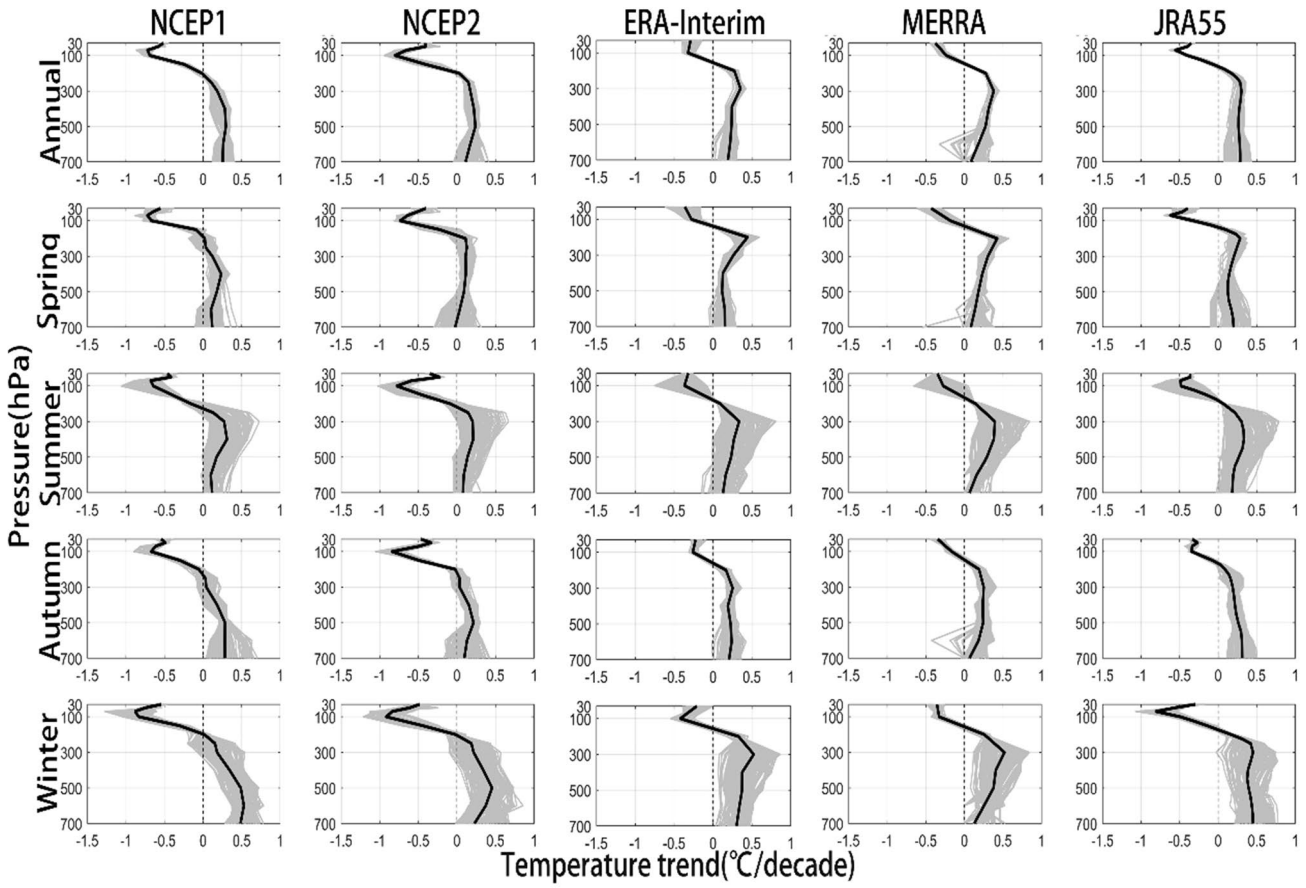

Fig. 3 Vertical profiles in temperature trends for each reanalysis (NCEP1, NCEP2, ERA-Interim, MERRA and JRA55) over the Tibetan Plateau during 1979–2018 on an annual and seasonal basis. Other comments are the same as Fig. 2

the exact position of the surface station both horizontally (between reanalysis grid points) and vertically. The comparison of observed data with interpolated data from nearest four grid points is widely used in climate change studies (Ahmed et al. 2019; Angélil et al. 2016).

After horizontal interpolation, the temperature from each reanalysis is corrected vertically to the real station height assuming a linear lapse rate derived from the reanalysis. The elevation correction is described:

$$T_1 = T_0 + \Gamma(z_1 - z_2) \quad (1)$$

where T_0 and T_1 is the surface temperature before and after elevation correction. z_2 and z_1 are the model and station elevations. Γ the temperature lapse rate estimated from the observations at each station in each year (month and season) for each reanalysis. Thus the lapse rate used for correction varies by station location, season and reanalysis. To calculate the Γ, the mean temperature profiles (Fig. 2) from each reanalysis (NCEP1, NCEP2, ERA-Interim, MERRA and JRA55) over the TP during 1979–2018 on an annual and seasonal basis are used. All profiles are broadly similar and reflect the current stratification of the atmosphere over the TP (Fig. 2), consistent with observed profiles at radiosonde stations over the TP (You et al. 2019b).

Examination of temperature trends in the vertical profile shows differential warming/cooling patterns below/above 300 hPa (Fig. 3), thus suggesting that the lapse rate below 300 hPa can be considered as a threshold to be used for the elevation correction process. The Γ above each station interpolated within each reanalysis on the annual and seasonal basis is calculated based on temperature and geopotential values between the ground level and 300 hPa, which can largely remove the influence of topographic characteristics, the synoptic circulation and atmospheric structure (Gao et al. 2012, 2017). Thus the selection of 300 hPa is better to employ the "closest" pressure level from the observations to calculate the lapse rate. Spatial patterns and time series of annual and seasonal mean Γ over the TP during 1979–2018 from the multiple reanalyses are plotted in Figs. 4 and 5 respectively, and it is clear that mean Γ has strongest values in spring (Fig. 4), and inter-annual variations (Fig. 5).

To assess the success of the elevation correction, the root mean square error (RMSE) is calculated before and after correction as:RMSE $= \sqrt{\frac{1}{n}\sum_{i=1}^{i=n}\left(T - T_{obs}\right)^2}$, where T rep-

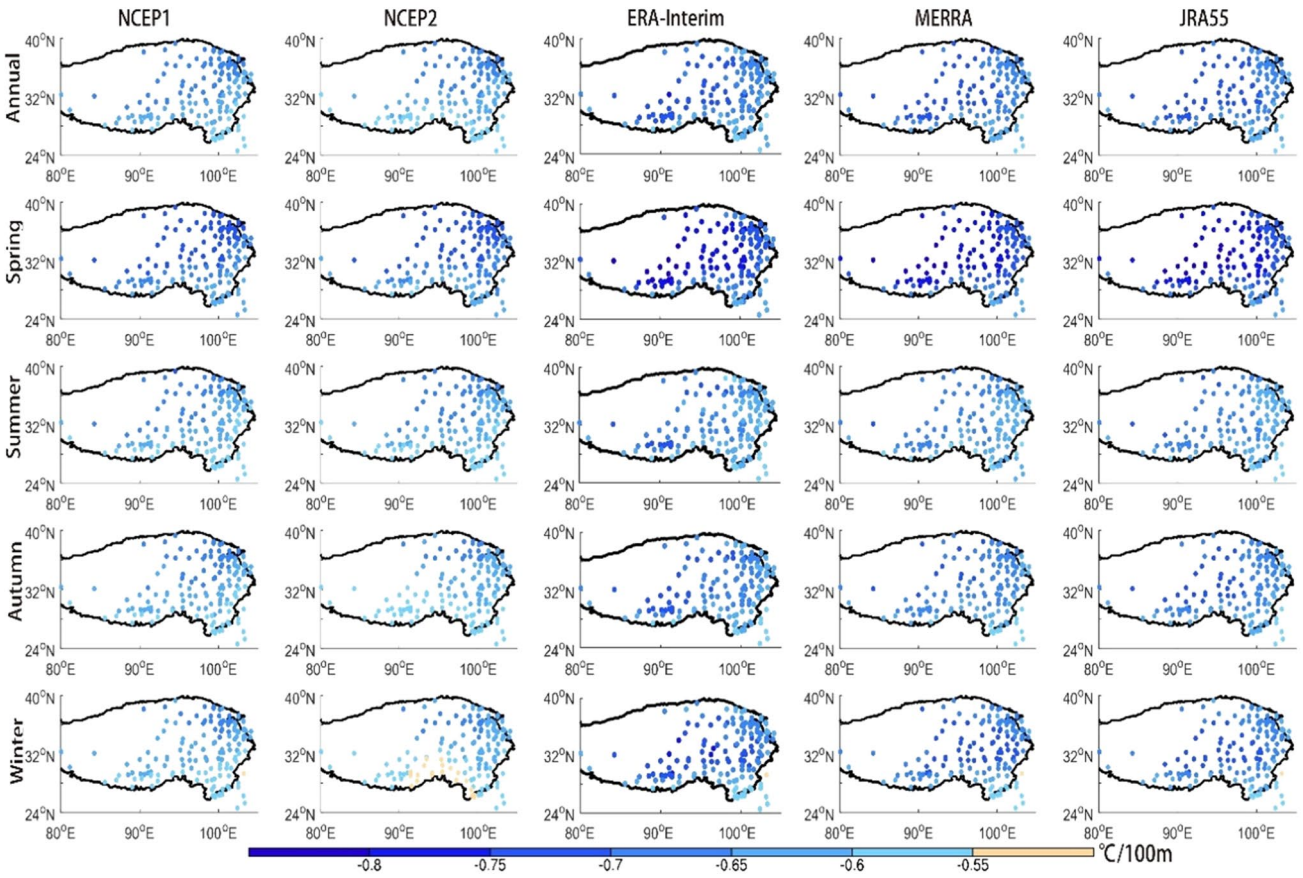

Fig. 4 Spatial patterns of temperature lapse rates from multiple reanalyses (NCEP1, NCEP2, ERA-Interim, MERRA and JRA55) over the Tibetan Plateau during 1979–2018 on an annual and seasonal basis

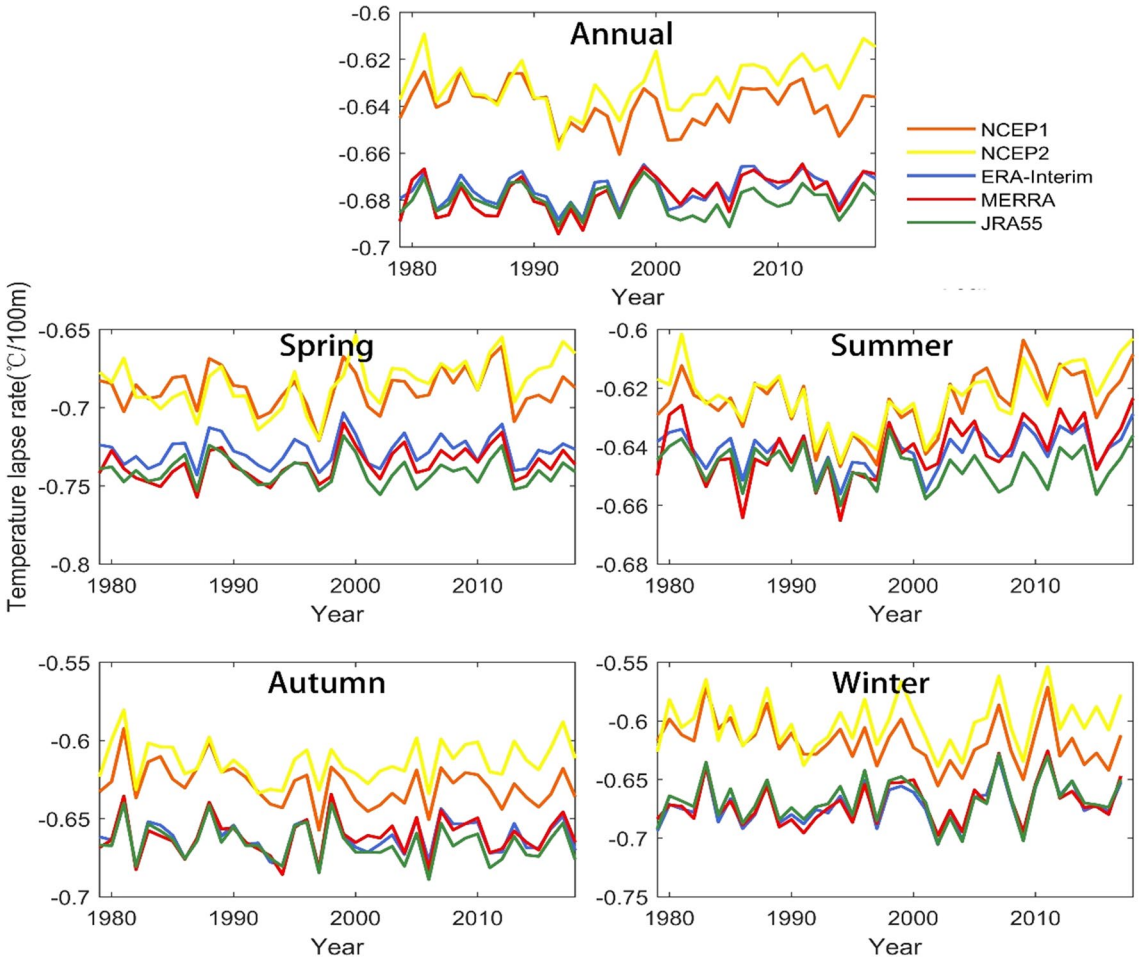

Fig. 5 Time series of temperature lapse rates from multiple reanalyses (NCEP1, NCEP2, ERA-Interim, MERRA and JRA55) over the Tibetan Plateau during 1979–2018 on an annual and seasonal basis

resents corrected surface temperature of each reanalysis in turn, T_{obs} is the corresponding station and N is the number of grid points (n = 150). Taylor diagrams are used to provide a concise statistical summary of how well patterns in datasets match each other in terms of their correlation, RMSE and the ratio of their variances (Taylor 2001).The Mann–Kendall test and Sen's slope estimates (Sen 1968) are used to determine trends in surface mean temperature from both the observations and reanalyses. We calculate both annual and seasonal trends (winter: DJF; spring: MAM; summer: JJA; autumn: SON) (Sen 1968).

3 Results

3.1 Warming patterns from the observations and multiple reanalyses

Table 2 summarizes annual and seasonal mean temperatures, their trends, absolute bias, RMSE, and percentage of improvement after calibration of each reanalysis over the TP during 1979–2018. The spatial distributions of surface temperature and differences in the surface temperature climatology between each reanalysis (uncorrected) and the observations are also presented in Fig. 6. On an annual basis, all reanalyses underestimate the observations (Fig. 6), but each shows a sensible seasonal cycle. The smallest differences occur in summer, but the largest occur in various seasons. Both MERRA and JRA55 appear closest to the observations. NCEP1 has the largest biases.

Time series of mean regional (plateau-wide) surface temperature from both the observations and corrected reanalyses show significant rapid warming during 1979–2018 (Fig. 7). Over the whole period, warming is common in both the observations and corrected reanalyses on an annual and seasonal basis, with most warming usually in winter (Table 2). Examining spatial patterns in more detail, the majority of individual stations shows an increase in surface temperature particularly for the observations (Table 2 and Fig. 8). Stations in the northern TP

Table 2 Annual and seasonal surface mean temperature climatologies (a), trends (b), absolute bias (c), and root mean square error (RMSE) (d) for station observations, raw and corrected reanalyses (NCEP1, NCEP2, ERA-Interim, MERRA, JRA55) over the Tibetan Plateau during 1979–2018

	Annual	Spring	Summer	Autumn	Winter
(a) Mean surface temperature (°C)					
Observation	5.15	5.76	13.85	5.38	−4.38
Raw					
NCEP1	0.91	0.77	10.24	1.38	−8.74
NCEP2	0.73	0.93	10.57	0.81	−9.39
ERA-Interim	2.30	2.45	11.06	2.61	−6.90
MERRA	2.45	2.88	11.17	2.68	−6.93
JRA55	2.43	2.94	11.08	2.68	−6.96
After correction					
NCEP1	3.80	3.89	13.07	4.21	−5.97
NCEP2	2.95	3.36	12.77	2.95	−7.29
ERA-Interim	5.84	6.27	14.40	6.07	−3.36
MERRA	6.23	7.01	14.72	6.36	−3.16
JRA55	5.99	6.83	14.45	6.16	−3.45
(b) Trend (°C/decade)					
Observation	**0.46**	**0.42**	**0.42**	**0.46**	**0.57**
Raw					
NCEP1	**0.26**	0.15	**0.13**	**0.28**	**0.51**
NCEP2	0.01	−0.17	0.08	0.01	0.08
ERA-Interim	**0.29**	**0.28**	**0.31**	**0.31**	**0.39**
MERRA	**0.27**	**0.24**	**0.23**	**0.27**	**0.39**
JRA55	**0.34**	**0.32**	**0.37**	**0.37**	**0.41**
After correction					
NCEP1	**0.27**	0.13	**0.10**	**0.28**	**0.55**
NCEP2	0.00	−0.19	0.07	−0.01	0.07
ERA-Interim	**0.28**	**0.27**	**0.30**	**0.30**	**0.37**
MERRA	**0.26**	**0.22**	**0.20**	**0.26**	**0.36**
JRA55	**0.34**	**0.30**	**0.37**	**0.38**	**0.41**
(c) Absolute Bias (°C)					
Raw					
NCEP1	−4.24	−4.98	−3.61	−4.01	−4.36
NCEP2	−4.42	−4.82	−3.27	−4.57	−5.01
ERA-Interim	−2.85	−3.31	−2.79	−2.77	−2.53
MERRA	−2.71	−2.87	−2.68	−2.71	−2.55
JRA55	−2.72	−2.82	−2.76	−2.70	−2.59
After correction					
NCEP1	−1.36	−1.88	−0.77	−1.18	−1.62
NCEP2	−2.22	−2.41	−1.07	−2.44	−2.94
ERA-Interim	0.69	0.51	0.55	0.69	1.02
MERRA	1.07	1.24	0.88	0.97	1.19
JRA55	0.83	1.06	0.61	0.77	0.89
(d) RMSE					
Raw					
NCEP1	4.27	5.02	3.62	4.03	4.41
NCEP2	4.48	4.93	3.30	4.62	5.10
ERA-Interim	2.87	3.32	2.79	2.79	2.57
MERRA	2.73	2.90	2.69	2.73	2.61
JRA55	2.74	2.83	2.76	2.71	2.63
After correction					
NCEP1	1.40	1.95	0.88	1.21	1.67
NCEP2	2.32	2.61	1.18	2.52	3.04

Table 2 (continued)

	Annual	Spring	Summer	Autumn	Winter
ERA-Interim	0.72	0.55	0.60	0.73	1.04
MERRA	1.11	1.28	0.95	1.03	1.25
JRA55	0.85	1.07	0.62	0.79	0.92
Percentage of improvement after correction					
NCEP1	67.10%	61.19%	75.71%	69.87%	62.20%
NCEP2	48.25%	46.98%	64.31%	45.43%	40.26%
ERA-Interim	74.91%	83.43%	78.49%	73.84%	59.53%
MERRA	59.22%	55.82%	64.74%	62.39%	51.99%
JRA55	69.11%	62.07%	77.54%	70.99%	64.87%

Significant trends are marked in bold ($p < 0.05$). The percentage reduction in RMSE after correction is also listed. Bias is defined as Reanalysis − Observation

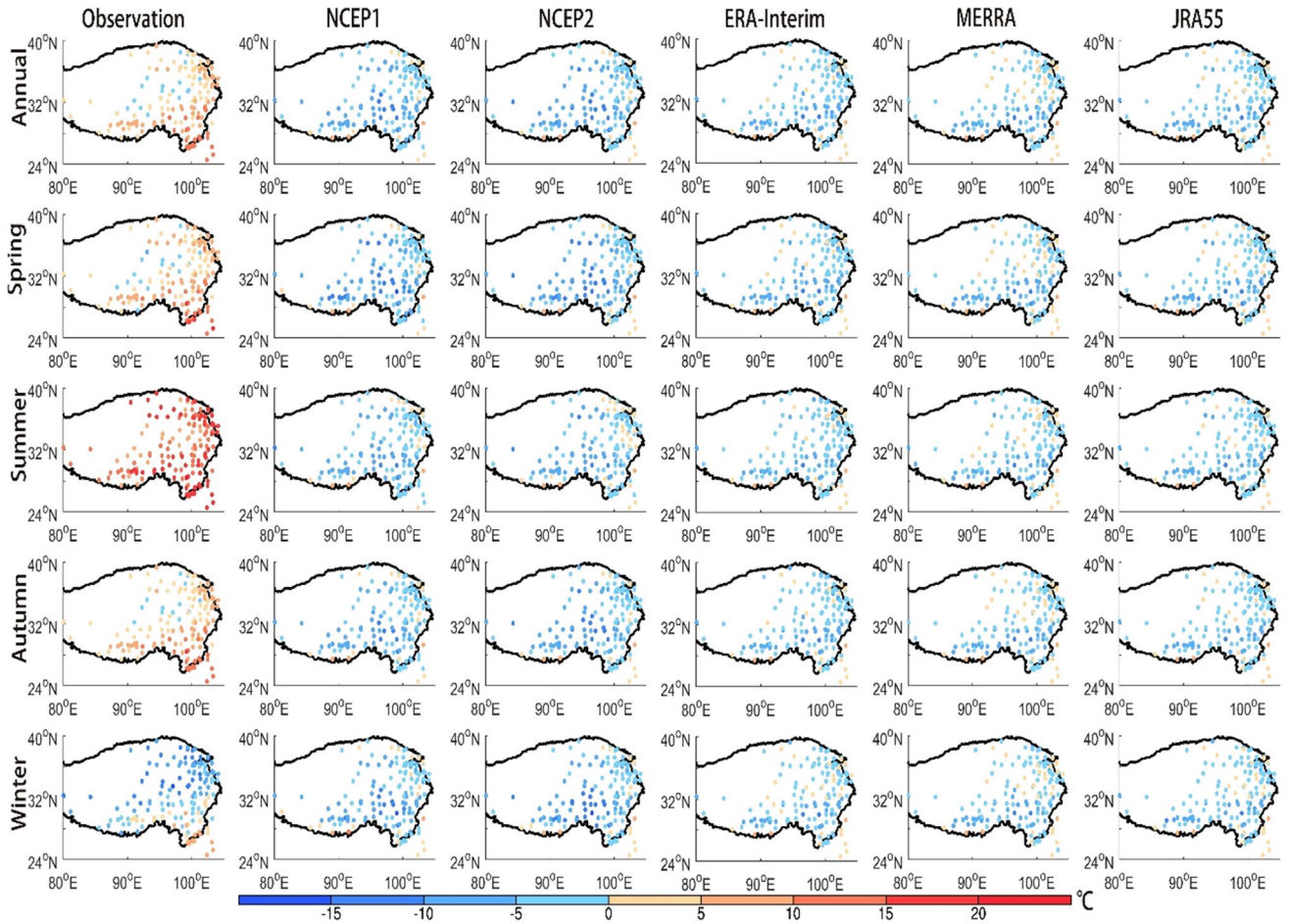

Fig. 6 Spatial distribution of climatological surface mean temperature from the observations (left column) and the difference (ΔT) between each reanalysis (NCEP1, NCEP2, ERA-Interim, MERRA and JRA55) and the observation before correction on an annual and seasonal basis. The unit is °C

tend to have larger trend magnitudes (You et al. 2008a, b). It is also clear that all reanalyses with the exception of NCEP2, show very similar trends to the observations during 1979–2018, suggesting that they can reproduce decadal variations in surface temperature in most cases (Figs. 7 and 8). With the exception of NCEP2, most reanalyses show a dominance of warming trends with the most pronounced warming in winter (Table 2). NCEP2,

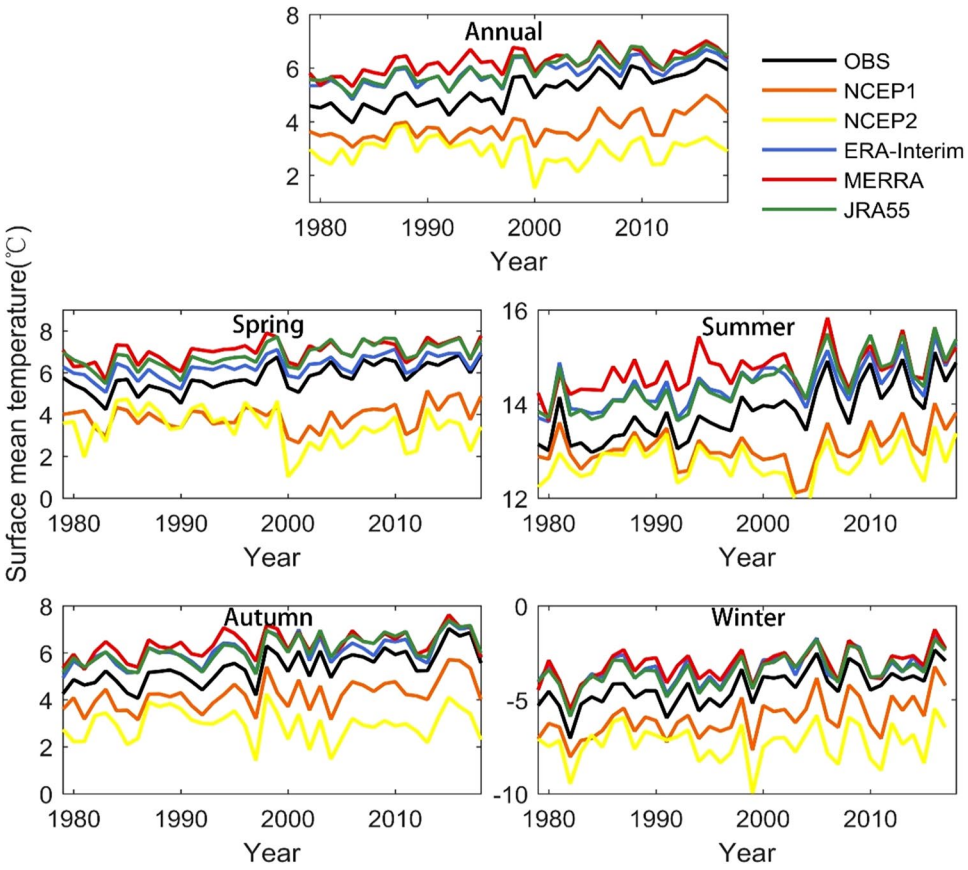

Fig. 7 Time series of regional surface mean temperature from the observations and each reanalysis (NCEP1, NCEP2, ERA-Interim, MERRA and JRA55) after horizontal bilinear interpolation and correction by elevation bias over the Tibetan Plateau during 1979–2018 on an annual (top panel) and seasonal basis (other four panels)

and to a lesser extent NCEP1, have negative trends at many stations, which are inconsistent with the observations. The other reanalyses appear to capture the main spatial patterns of warming over the TP, although there are some differences in trend magnitudes in individual seasons between the observations and individual reanalyses (Fig. 8).

3.2 Evaluation of the elevation-correction for multiple reanalyses

We examined the relationship between temperature bias and elevation bias (reanalysis minus observation). In most cases, elevation differences (model minus surface station elevation, ΔH) are positive because surface stations are situated in flat areas and valley bottoms which tend to be lower than the reanalysis model topography (You et al. 2008b, 2013). This could explain a general underestimation of surface temperature in the reanalyses. Scatter plots of absolute errors (reanalysis minus observation) of mean surface temperature (ΔT) vs elevation (ΔH) for all 150 stations are presented in Fig. 9. There are highly significant negative correlations ($p < 0.01$) both on an annual basis and in all seasons showing that underestimation of surface temperature in all reanalyses is mainly explained by the overestimation of the elevation in the model assimilations (highest correlations are for ERA-Interim and JRA55).

Because much of the surface temperature bias between the observations and reanalyses is explained by elevation differences, this confirms the importance of our correction procedures (Gao et al. 2017; Song et al. 2016; Zhao et al. 2008). Spatial distribution of mean absolute biases after correction (reanalysis minus observation) of surface temperature over the TP on an annual and seasonal basis is shown in Fig. 10, and the percentage of improvement after correction is summarized in the bottom rows of Table 2.

Dramatic improvements are achieved through elevation correction with errors of all reanalysis datasets reduced by more than 50%. After the correction, NPCE1 and NCEP2 still retain a cold bias, but the rest (ERA-Interim, MERRA and JRA 55) show warm bias (Fig. 10 and Table 2). The best result is for ERA-Interim whose error is reduced by > 74%, closely followed by JRA55 (> 69%) and NCEP1 (> 60%) (Table 2). The correction process was slightly more successful in summer, agreeing with other studies (Zhao et al. 2008). Temperature inversions in winter may make a correction based on a simple lapse rate slightly less effective (Wang et al. 2015; You et al. 2017, 2019b).

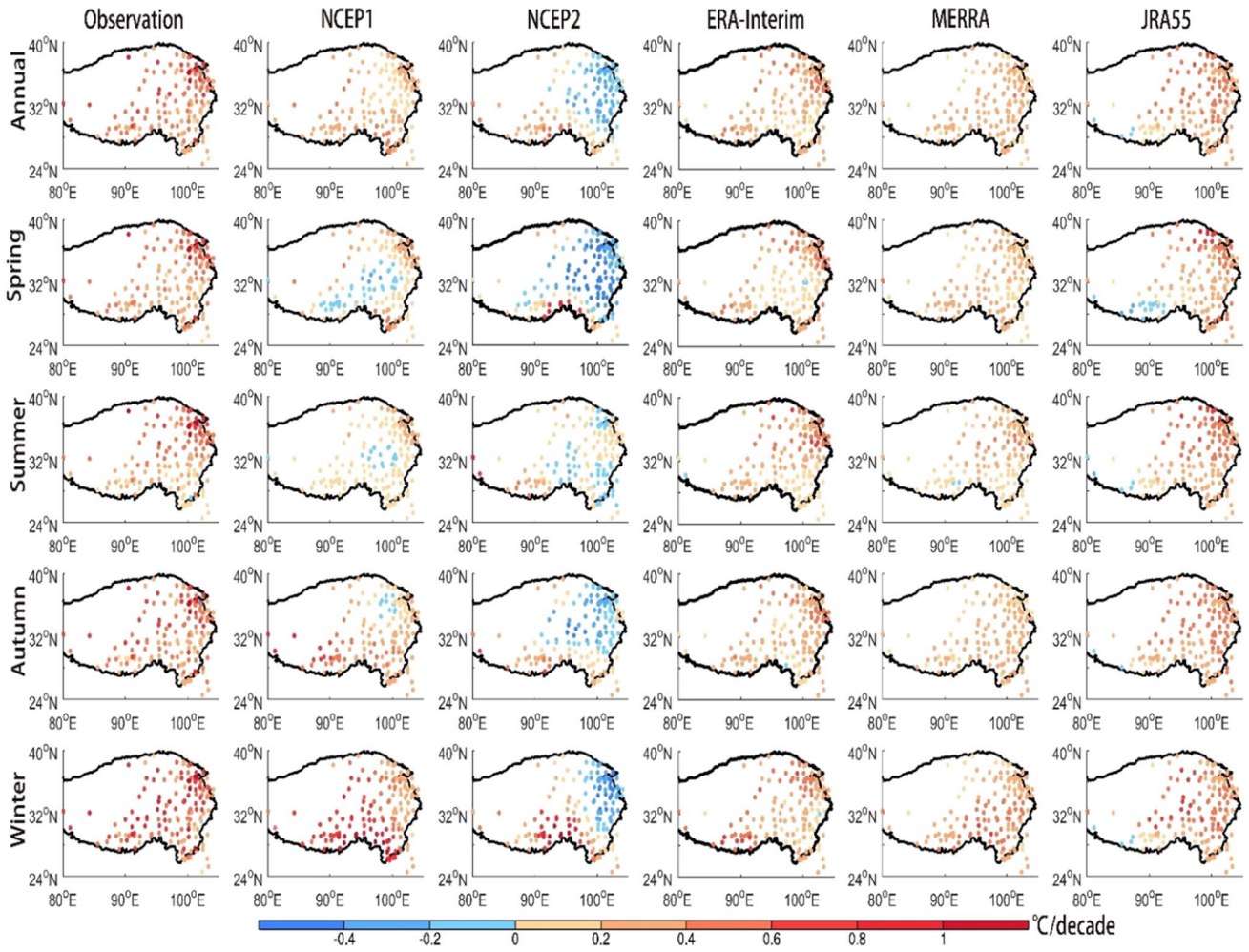

Fig. 8 Spatial distribution of trend of surface mean temperature from the observation and each reanalysis (NCEP1, NCEP2, ERA-Interim, MERRA and JRA55) after correction for elevation difference over the Tibetan Plateau during 1979–2018 on an annual and seasonal basis. The unit is °C/decade. Solid/hollow triangles are stations with trends which pass/fail the significance test ($p < 0.05$)

3.3 Discussion and conclusions

Based on historical surface air temperature records at 150 meteorological stations over the TP during 1979–2018, temperature trends have been investigated and compared with those from reanalyses interpolated to the same locations (NCEP1, NCEP2, ERA-Interim, MERRA, JRA55). Results indicate that observed warming over the TP is significant since 1979 with a mean annual rate of 0.46 °C/decade particularly in winter, which is larger than the whole of China, regions between 25° and 40° N, the Northern Hemisphere and the global mean (Fig. 11), suggesting that the TP is a sensitive region to global and regional climate change, probably due to the coexistence of glaciers, lakes, permafrost, alpine meadows and other natural elements (Kang et al. 2010; Yao et al. 2019; You et al. 2013). The rapid warming has persisted over the TP during the global warming hiatus period. The revealed rapid warming over the TP is consistent with recent studies (Cai et al. 2017; Duan and Xiao 2015; Rangwala and Miller 2012; Rangwala et al. 2013; You et al. 2016, 2017), although the trend magnitudes of this study are larger than the previous research. The significant warming signature over the TP is significant and present in the observations and the corrected reanalyses, and the mean of corrected reanalyses over the TP has a mean annual rate of 0.23 °C/decade during 1979–2018 (Fig. 11). This suggests that mean of corrected reanalyses underestimates 50% of the annual trend magnitude derived from the observations, and the corrected reanalyses captures the overall warming over the TP but fails to reproduce the pronounced warming in this region. Possible factors such as snow-albedo feedback, cloud-radiation feedback and atmospheric circulation are analyzed to determine the recent climate warming over the TP, and consensus about relative importance of these factors is low (Duan and Wu 2006; Duan et al. 2006; Kang et al. 2019; Yang et al. 2019; You et al. 2016, 2010a, b, 2020a, b).

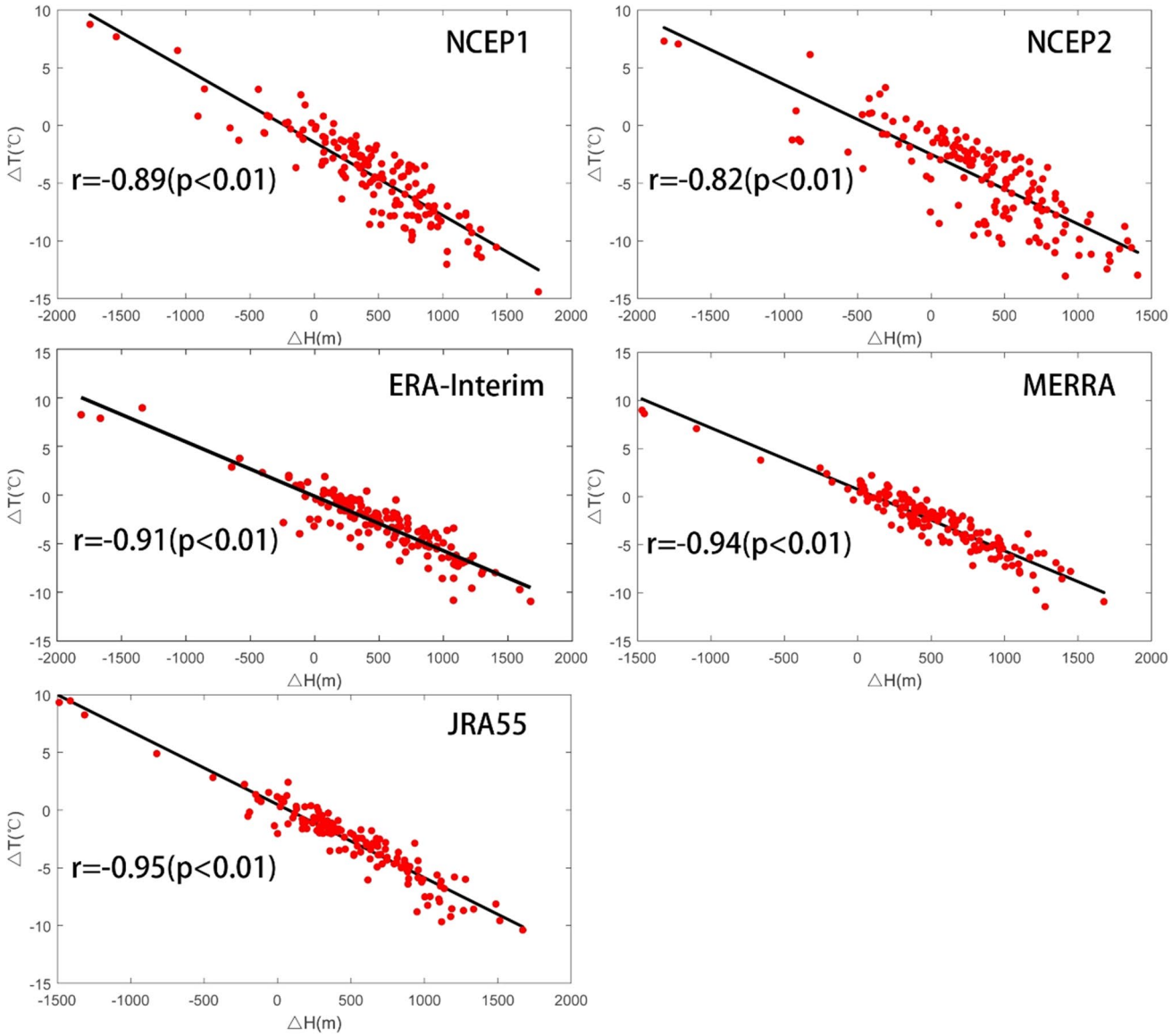

Fig. 9 Scatter plots of normalized absolute error (reanalysis minus observation) of surface mean temperature (ΔT) versus elevation error (ΔH) for each reanalysis

For example, the increase in nocturnal low-level cloud and the decrease of daytime low and total cloud amounts over the TP, will result in more absorbing of direct solar radiation at the surface and contribute to the increased surface air temperature over the TP to some extents (Duan and Wu 2006; Duan et al. 2006).

Although surface temperature from reanalyses (NCEP1, NCEP2, ERA-Interim, MERRA, JRA55) can capture much of the inter-decadal variability of in situ station surface temperatures, there are consistent negative biases. Since there are significant negative correlations between this bias and elevation error (reanalysis minus observation) on both an annual and seasonal basis, we correct the reanalyses to remove most of the surface temperature biases, as has been done in other studies over the TP (You et al. 2013) and in eastern China (Ma et al. 2008). Around 40–70% of the mean bias is eliminated through elevation correction. However, it is addressed that the bias from reanalyses can be caused by some important parameterization schemes, the amplification of the false changes introduced by the observation, the deficiencies of the physical process in the numerical prediction model and assimilation scheme (Kalnay et al. 1996; Kanamitsu et al. 2002). This suggests that the elevation correction methods cannot completely remove all biases in reanalyzes. For example, even after elevation correction, both NCEP1 and NCEP2 still

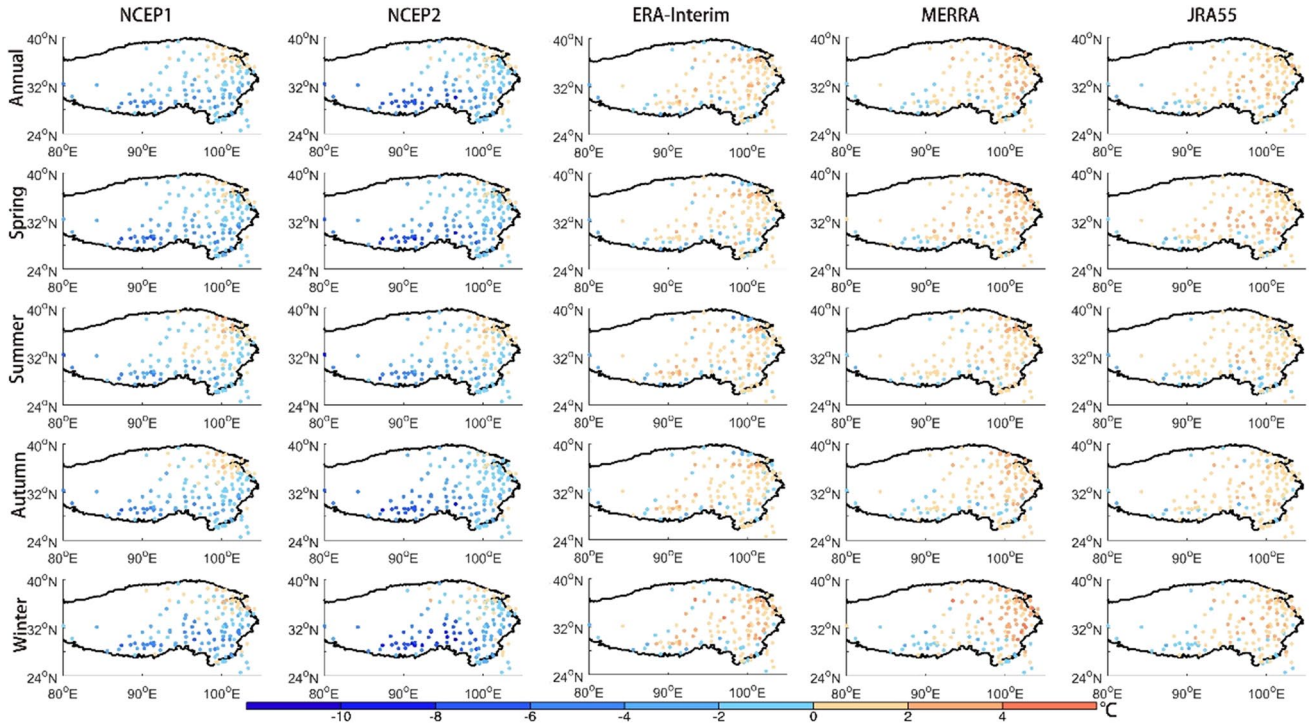

Fig. 10 Spatial distribution of mean absolute bias (corrected reanalysis minus observation) of surface mean temperature over the Tibetan Plateau on an annual and seasonal basis. The unit is °C

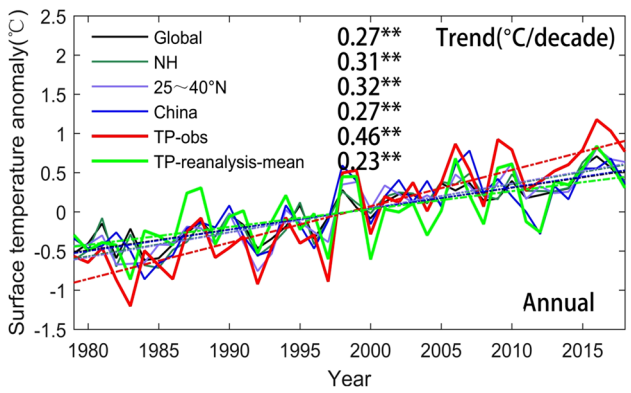

Fig. 11 Time series and trends of annual surface mean temperature anomalies during 1979–2018 over the Tibetan Plateau (TP, TP-obs and TP-reanalysis-mean), the whole of China, regions between 25° and 40° N, the Northern Hemisphere (NH), and the global mean. Data of TP-obs and TP-reanalysis-mean come from the observations and the mean of corrected reanalyses (NCEP1, NCEP2, ERA-Interim, MERRA and JRA55). Other dataset are derived from the High-resolution gridded dataset CRU TS v.4.03 (https://www.cru.uea.ac.uk). The trends passed the significant test ($p < 0.05$) are marked by double asterisks

have some cold biases. Although NCEP2 has improved assimilation methods in comparison with NCEP1, the surface mean temperature in NCEP2 still does not perform well over the TP. For example minimum temperatures in NCEP2 have a − 12 °C cold bias in winter (Mao et al. 2010). Previous studies have indicated that the evaluation and correction of reanalysis datasets is crucial before they can be applied in climate research (Duan and Xiao 2015; Ma et al. 2008; Mao et al. 2010; Wang et al. 2015; Yang and Zhang 2018). More attention to such issues should be given when examining trends over the TP from different sources, since topographical differences between grid points and station locations (in addition to elevation) may also influence trend magnitudes and patterns (You et al. 2013).

Separate Taylor diagrams are shown for annual and seasonal surface mean temperature from the observation and corrected multiple reanalyses over the TP (Fig. 12). All the corrected reanalyses over the TP have good spatial correlations with the observations with the correlation over 0.8 (with the exception of NCEP2) and normalized standardized deviations between 0.5 and 1, indicating the corrected reanalyses perform relatively well the overall patterns of surface mean temperature over the TP, although the inconsistencies existing between the corrected reanalyses for trend analysis. Meanwhile, the results of the elevation correction vary between seasons. It is generally less successful in winter because surface based temperature inversions are not modeled well, using a linear lapse rate between the surface level and 300 hPa. In summer the well-mixed atmosphere means that a simple elevation

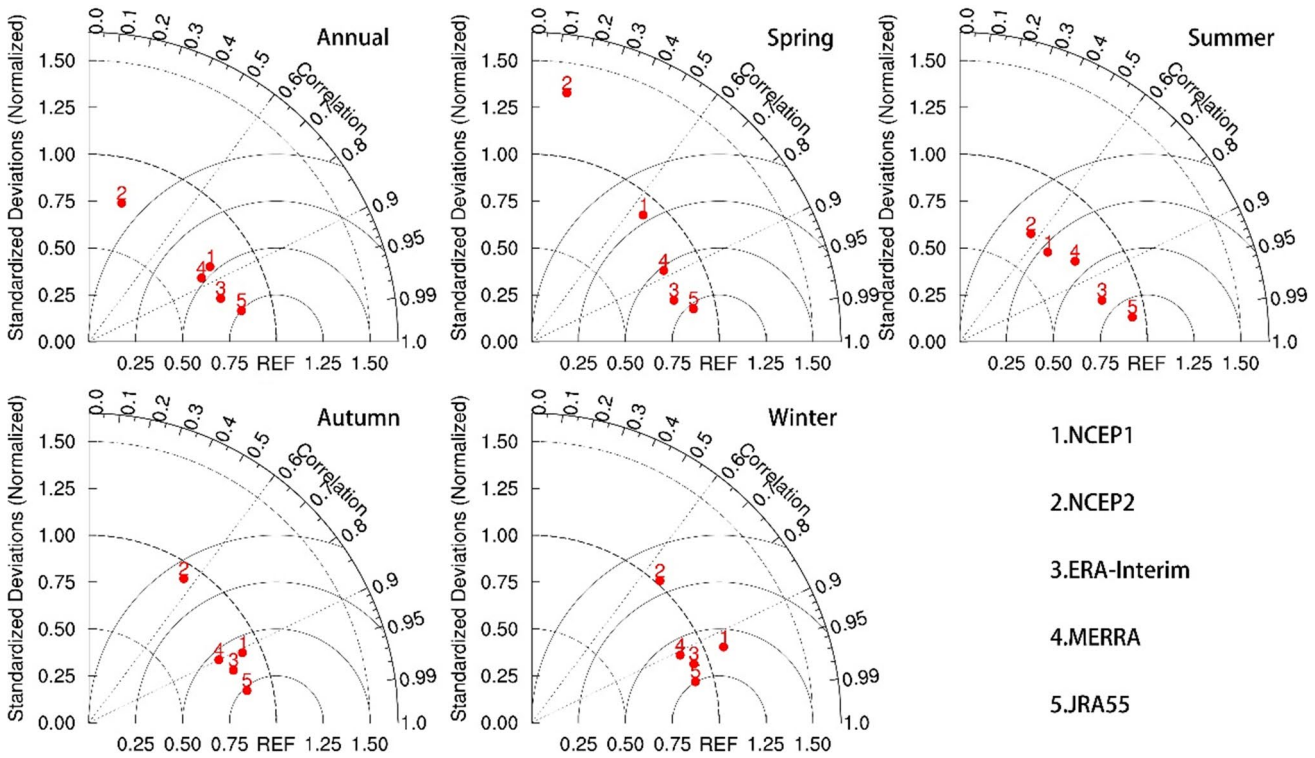

Fig. 12 Taylor diagrams showing the evaluation metrics between mean annual and seasonal surface mean temperature from the observations and corrected multiple reanalyses over the Tibetan Plateau during 1979–2018. Numbers 1–5 represent NCEP1, NCEP2, ERA-Interim, MERRA and JRA55, respectively. The correlation coefficients and normalized standard deviation are also shown. The REF is recognized as the observations, and the normalized root mean square error is the distance between the REF and each reanalysis

correction works more effectively. There are also differences between reanalyses. Significant improvements for JRA55, ERA-Interim and MERRA are clear and closer to the observations (Fig. 12), but improvements are much weaker for NCEP1 and NCEP2 because the "surface" temperature in both reanalyses is more dependent on free-air forcing, and surface observations are not assimilated (Simmons et al. 2004).

We have used a seasonally and spatially variable lapse rate of air temperature for our correction, deduced from temperature and geopotential height between the surface and 300 hPa. In reality there are complex spatial and temporal variations in lapse rate (Wang et al. 2018). Recently, some studies using ERA-Interim have included model internal vertical lapse rates derived from different pressure levels to validate surface temperatures from meteorological stations, and they indicate that the use of model variable rates can significantly improve downscaling performance (Gao et al. 2012, 2017; Luo et al. 2019; Zou et al. 2014). Future research should therefore focus on the calculation of internal vertical lapse rates derived from pressure levels in each reanalysis, and more high resolution of reanalysis such as ERA-5 should be applied to further this study.

Acknowledgements This study is supported by the Second Tibetan Plateau Scientific Expedition and Research (SETP) Program (Grant no. 2019QZKK0103) and National Natural Science Foundation of China (41771069 and 41971072). We are very grateful to the reviewers for their constructive comments and thoughtful suggestions.

References

Ahmed K, Shahid S, Wang X, Nawaz N, Khan N (2019) Evaluation of gridded precipitation datasets over arid regions of Pakistan. Water 11:210

Angélil O et al (2016) Comparing regional precipitation and temperature extremes in climate model and reanalysis products. Weather Clim Extremes 13:35–43

Cai D, You Q, Fraedrich K, Guan Y (2017) Spatiotemporal temperature variability over the Tibetan Plateau: altitudinal dependence associated with the global warming hiatus. J Clim 30:969–984

Dee DP et al (2011) The ERA-Interim reanalysis: configuration and performance of the data assimilation system. Q J R Meteorol Soc 137:553–597

Duan AM, Wu GX (2006) Change of cloud amount and the climate warming on the Tibetan Plateau. Geophys Res Lett 33:L22704

Duan AM, Xiao ZX (2015) Does the climate warming hiatus exist over the Tibetan Plateau? Sci Rep 5:13711

Duan AM, Wu GX, Zhang Q, Liu YM (2006) New proofs of the recent climate warming over the Tibetan Plateau as a result

of the increasing greenhouse gases emissions. Chin Sci Bull 51:1396–1400
Frauenfeld OW, Zhang TJ, Serreze MC (2005) Climate change and variability using European Centre for Medium-Range Weather Forecasts reanalysis (ERA-40) temperatures on the Tibetan Plateau. J Geophys Res Atmos 110:D02101
Gao L, Bernhardt M, Schulz K (2012) Elevation correction of ERA-Interim temperature data in complex terrain. Hydrol Earth Syst Sci 16:4661–4673
Gao L, Bernhardt M, Schulz K, Chen X (2017) Elevation correction of ERA-Interim temperature data in the Tibetan Plateau. Int J Climatol 37:3540–3552
Guo D, Yu E, Wang H (2016a) Will the Tibetan Plateau warming depend on elevation in the future? J Geophys Res Atmos 121:3969–3978
Guo X, Wang L, Tian L (2016b) Spatio-temporal variability of vertical gradients of major meteorological observations around the Tibetan Plateau. Int J Climatol 36:1901–1916
Immerzeel WW, van Beek LPH, Bierkens MFP (2010) Climate change will affect the Asian water towers. Science 328:1382–1385
Ji Z, Kang S (2013a) Projection of snow cover changes over China under RCP scenarios. Clim Dyn 41:589–600
Ji Z, Kang S (2013b) Double-nested dynamical downscaling experiments over the Tibetan Plateau and their projection of climate change under two RCP scenarios. J Atmos Sci 70:1278–1290
Kalnay E et al (1996) The NCEP/NCAR 40-year reanalysis project. Bull Am Meteorol Soc 77:437–471
Kanamitsu M, Ebisuzaki W, Woollen J, Yang SK, Hnilo JJ, Fiorino M, Potter GL (2002) NCEP-DOE AMIP-II reanalysis (R-2). Bull Am Meteorol Soc 83:1631–1643
Kang SC, Xu YW, You QL, Flugel WA, Pepin N, Yao TD (2010) Review of climate and cryospheric change in the Tibetan Plateau. Environ Res Lett 5:015101
Kang SC et al (2019) Linking atmospheric pollution to cryospheric change in the Third Pole region: current progress and future prospects. Natl Sci Rev 6:796–809
Kistler R et al (2001) The NCEP-NCAR 50-year reanalysis: monthly means CD-ROM and documentation. Bull Am Meteorol Soc 82:247–267
Kobayashi S et al (2015) The JRA-55 reanalysis: general specifications and basic characteristics. J Meteor Soc Japan 93:5–48
Kuang X, Jiao J (2016) Review on climate change on the Tibetan Plateau during the last half century. J Geophys Res Atmos 121:3979–4007
Li QX, Huang J, Jiang Z, Zhou L, Chu P, Hu K (2014) Detection of urbanization signals in extreme winter minimum temperature changes over Northern China. Clim Change 122:595–608
Liu XD, Yin ZY, Shao XM, Qin NS (2006) Temporal trends and variability of daily maximum and minimum, extreme temperature events, and growing season length over the eastern and central Tibetan Plateau during 1961–2003. J Geophys Res Atmos 111:D19109
Liu XD, Cheng Z, Yan L, Yin Z-Y (2009) Elevation dependency of recent and future minimum surface air temperature trends in the Tibetan Plateau and its surroundings. Glob Planet Change 68:164–174
Luo H et al (2019) Assessment of ECMWF reanalysis data in complex terrain: can the CERA-20C and ERA-Interim data sets replicate the variation in surface air temperatures over Sichuan, China? Int J Climatol 39:5619–5634
Ma LJ, Zhang TJ, Li QX, Frauenfeld OW, Qin DH (2008) Evaluation of ERA-40, NCEP-1, and NCEP-2 reanalysis air temperatures with ground-based measurements in China. J Geophys Res Atmos 113:D15115
Mao J, Shi X, Ma L, Kaiser DP, Li Q, Thornton PE (2010) Assessment of reanalysis daily extreme temperatures with China's homogenized historical dataset during 1979–2001 using probability density functions. J Clim 23:6605–6623
Qin J, Yang K, Liang SL, Guo XF (2009) The altitudinal dependence of recent rapid warming over the Tibetan Plateau. Clim Change 97:321–327
Qiu J (2008) The Third pole. Nature 454:393–396
Rangwala I, Miller JR (2012) Climate change in mountains: a review of elevation-dependent warming and its possible causes. Clim Change 114:527–547
Rangwala I, Sinsky E, Miller JR (2013) Amplified warming projections for high altitude regions of the northern hemisphere mid-latitudes from CMIP5 models. Environ Res Lett 8:024040
Rienecker MM et al (2011) MERRA: NASA's modern-era retrospective analysis for research and applications. J Clim 24:3624–3648
Sen PK (1968) Estimates of regression coefficient based on Kendall's tau. J Am Stat Assoc 63:1379–1389
Simmons AJ et al (2004) Comparison of trends and low-frequency variability in CRU, ERA-40, and NCEP/NCAR analyses of surface air temperature. J Geophys Res Atmos 109:D24115
Smith T, Bookhagen B (2018) Changes in seasonal snow water equivalent distribution in High Mountain Asia (1987 to 2009). Sci Adv 4:e1701550
Song CQ, Ke LH, Richards KS, Gui YZ (2016) Homogenization of surface temperature data in High Mountain Asia through comparison of reanalysis data and station observations. Int J Climatol 36:1088–1101
Taylor KE (2001) Summarizing multiple aspects of model performance in a single diagram. J Geophys Res Atmos 106:7183–7192
Wang S, Zhang M, Sun M, Wang B, Huang X, Wang Q, Feng F (2015) Comparison of surface air temperature derived from NCEP/DOE R2, ERA-Interim, and observations in the arid northwestern China: a consideration of altitude errors. Theor Appl Climatol 119:99–111
Wang T, Sun F, Ge Q, Kleidon A, Liu W (2018) The effect of elevation bias in interpolated air temperature data sets on surface warming in china during 1951–2015. J Geophys Res Atmos 123:2141–2151
Xu Y, Gao XJ, Yan SY, Xu CH, Shi Y, Giorgi F (2009) A daily temperature dataset over China and its application in validating a RCM simulation. Adv Atmos Sci 26:763–772
Yan LB, Liu XD (2014) Has climatic warming over the Tibetan Plateau paused or continued in recent years? J Earth Ocean Atmos Sci 1:13–28
Yang K, Zhang J (2018) Evaluation of reanalysis datasets against observational soil temperature data over China. Clim Dyn 50:317–337
Yang M, Wang X, Pang G, Wan G, Liu Z (2019) The Tibetan Plateau cryosphere: Observations and model simulations for current status and recent changes. Earth Sci Rev 190:353–369
Yao T et al (2012) Different glacier status with atmospheric circulations in Tibetan Plateau and surroundings. Nat Clim Change 2:663–667
Yao T et al (2019) Recent Third Pole's rapid warming accompanies cryospheric melt and water cycle intensification and interactions between monsoon and environment: multi-disciplinary approach with observation, modeling and analysis. Bull Am Meteorol Soc 100:423–444
You QL, Kang SC, Aguilar E, Yan YP (2008a) Changes in daily climate extremes in the eastern and central Tibetan Plateau during 1961–2005. J Geophys Res Atmos 113:D07101
You QL, Kang SC, Pepin N, Yan YP (2008b) Relationship between trends in temperature extremes and elevation in the eastern and central Tibetan Plateau, 1961–2005. Geophys Res Lett 35:L04704
You QL, Kang SC, Pepin N, Flugel WA, Yan YP, Behrawan H, Huang J (2010a) Relationship between temperature trend magnitude, elevation and mean temperature in the Tibetan Plateau from

homogenized surface stations and reanalysis data. Glob Planet Change 71:124–133

You QL, Kang SC, Pepin N, Flugel WA, Sanchez-Lorenzo A, Yan YP, Zhang YJ (2010b) Climate warming and associated changes in atmospheric circulation in the eastern and central Tibetan Plateau from a homogenized dataset. Glob Planet Change 72:11–24

You QL, Fraedrich K, Ren G, Pepin N, Kang S (2013) Variability of temperature in the Tibetan Plateau based on homogenized surface stations and reanalysis data. Int J Climatol 33:1337–1347

You QL, Min J, Kang S (2016) Rapid warming in the Tibetan Plateau from observations and CMIP5 models in recent decades. Int J Climatol 36:2660–2670

You QL, Jiang ZH, Moore G, Bao YT, Kong L, Kang SC (2017) Revisiting the relationship between observed warming and surface pressure in the Tibetan Plateau. J Clim 30:1721–1737

You QL, Zhang YQ, Xie X, Wu F (2019a) Robust elevation dependency warming over the Tibetan Plateau under global warming of 1.5 °C and 2 °C. Clim Dyn 53:2047–2060

You QL, Bao Y, Jiang Z, Pepin N, Moore GWK (2019b) Surface pressure and elevation correction from observation and multiple reanalyses over the Tibetan Plateau. Clim Dyn 53:5893–5908

You QL, Wu F, Shen L, Pepin N, Jiang Z, Kang S (2020a) Tibetan Plateau amplification of climate extremes under global warming of 1.5 °C, 2 °C and 3 °C. Glob Planet Change 192:103261

You QL et al (2020b) Review of snow cover variation over the Tibetan Plateau and its influence on the broad climate system. Earth Sci Rev 201:103043

Zhao T, Guo W, Fu C (2008) Calibrating and evaluating reanalysis surface temperature error by topographic correction. J Clim 21:1440–1446

Zou H, Zhu J, Zhou L, Li P, Ma S (2014) Validation and application of reanalysis temperature data over the Tibetan Plateau. J Meteorol Res 28:139–149